PLASMA, GASES

STABILITY OF AN ELECTRON BEAM WITH STRONG SPREAD OVER VELOCITIES IN A SELF-CONSISTENT PENNING—MALMBERG TRAP

V.I. LAPSHIN, I.K. TARASOV, I.V. TKACHENKO, V.I. TKACHENKO

Institute of Plasma Physics,
National Science Center "Kharkiv Institute of Physics and Technology"
(1, Academichna Str., Kharkiv 61108, Ukraine; e-mail: tkachenko@kipt.kharkov.ua)

A mechanism of electron plasma accumulation and confinement during the injection of an electron beam widely spread in the longitudinal velocity into a drift tube in a strong uniform magnetic field is studied both experimentally and theoretically. The properties and the formation of a collective electron trap for the electron beam that propagates in a conducting cylinder are described. It is experimentally shown that the electron beam stimulates the development of an instability under the above-mentioned conditions. The instability leads to the formation of an electric potential trap. The trap captures electrons during the formation and confines them inside the drift tube. The theoretical explanation of the last stage of the experiment (the confinement of charged particles) is given within the framework of the model considering the shearless motion of a tubular electron beam with constant density profile. The dispersion equation is obtained, and the conditions for the existence of the instability are elucidated. The results of numerical calculations are in good agreement with the experiment.

1. Introduction

The results obtained in the experiments on the cooling of a charged plasma and a plasma which consists of particles of the same sign of charge indicate the relative simplicity of its long-term confinement by external electromagnetic fields [1, 2]. The examinations of the relaxation of a bounded electron plasma to an equilibrium state and the dynamics of its parameters show that the force which restricts a motion of particles along a magnetic field should not be necessarily external. It may be self-consistent and appear as a result of various dynamic processes accompanying, in our case, the streaming of the charged plasma as a beam of charged particles spread over velocities in a magnetic field. It is known that the injection of a "hot" beam of charged particles with a wide spread of velocities in the vacuum channel of drift is accompanied by the conversion of the mono-flux motion of particles to the multi-flux one. It is related to the appearance of an electrostatic potential well at the stage preceding to the formation of an anticathode. It follows from the experimental results that the potential well had two maxima [3]. Such spatial distribution of electrical and magnetic fields represents an analog of the Penning—Malmberg trap, being a result of the dynamics of beam particles in the drift space [4]. The experiments also have shown that the electron plasma has a rather low temperature in the drift space in the area between two maxima of the potential well. The density of the accumulated electron plasma differs from that of the basic drifting stream in the course of time by an order of magnitude. The lifetime of accumulated particles exceeds the transition time of basic ones by 5—6 orders of magnitude.

For studying the questions of the accumulation and the long-term confinement of charged particles in Penning—Malmberg traps, it is necessary to build up a general stability theory of similar systems. The basic theoretical questions of stability for various types of traps are examined in [5]. In addition, for the last decade, a lot of theoretical publications considering how the various edge effects, such as the curvature of sheaths at the ends of the trap and the free boundary effect [6] or the end shape effects [7], influence the development
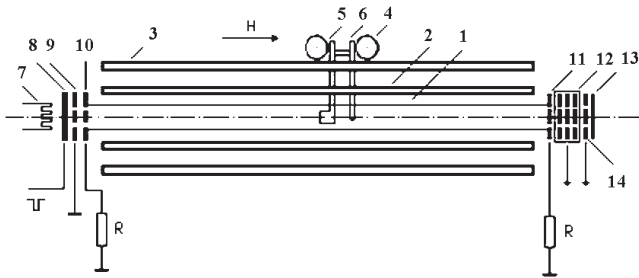
Fig. 1. Schematic of the experiment: *1* — electron beam; *2* — drift tube; *3* — intermediate wave guide; *4* — carriage; *5* — electrostatic analyzer; *6* — high-frequency probe; *7* —incandescent filament; *8* — heating cathode; *9* — anode grid; *10* — entrance grid; *11* — exit grid; *12* — electrostatic analyzer; *13* — collector grid; *14* — collector

Fig. 2. Current I_{ex} versus I_{in} for a pulsed beam with U_B=50 V, (τ: pulse duration, T: time between pulses). *1* — $\tau = 400$ μs, $T = 800$ μs, *2* — $\tau = 400$ μs, $T = 2.8$ ms

of instability have been published. In [8], the development of an instability of hollow electron beams has been qualitatively predicted. However, on the whole, such types of the formation are unstable with lifetimes equal to the time of the diocotron instability development τ_d. Here, we offer a physical model which allows us to give the explanation of the long-term confinement of a tubular electron beam.

2. Experimental Part

The experiments were performed in the device shown in Fig. 1 and described in detail in [9]. The hollow electron beam (the diameter a=2 cm, thickness $\Delta = 1 \div 2$ cm, and an energy of $20 \div 50$ eV) was injected into the drift space (the tube of the length $L \approx 150$ cm and the diameter $D = 4$ cm) which was limited from the edges by entrance and exit plane grids. The tube is cut longitudinally into two equal parts with an angular dimension of 180° (π-electrodes). The constant homogeneous longitudinal magnetic field has the strength of $H = 100 \div 1000$ Oe. The working pressure of the mixture (N_2, Ar) was 10^{-6}— 10^{-7} Torr. In the experiments, we determined the time-averaged distribution function over longitudinal energies with electrostatic analyzers; the particle density in the drift space by measuring the frequency of the diocotron mode with the azimuthal number l=1; the emission current of the electron gun cathode; the current I_{in} on the drift space electrode; the current I_{ex} on the exit; the oscillations and currents on HF probes; and the currents on π-electrodes.

In the experiments performed, a special attention was paid to analyzing the ion background formed by beam electrons ionizing the residual gas. In our experiments, the influence of the ion background arising from the ionization of the residual gas by beam electrons was not
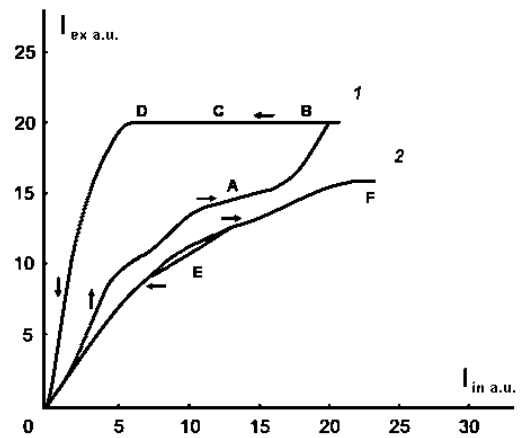
essential. In Fig. 2, we show the dependence of the current passed through the drift space I_{ex} on the current at the entrance I_{in}, when the voltage at the electron gun cathode is U=–50 V. It is seen from Fig. 2 that, as I_{in} increases, the movement along curve *1* from point *0* to point *B* is realized along its lower branch. When I_{in} decreases, the movement along the curve from *B* to *0* occurs along its upper branch. Thus, curve *1* of Fig. 2 exhibits a hysteresis on the dependence I_{ex} versus I_{in} which, however, is opposite in nature to the well-known similar hysteresis dependence for the monoenergetic beam [6] and the beam having a strong spread over longitudinal velocities, when they are in the stationary regime. Meanwhile, in curve *2* of Fig. 2, the hysteresis in I_{ex} versus I_{in} dependence is absent. Curve *2* differs from curve *1* only in the delay time between two subsequent periodic current pulses. This time is 3.5 times larger for curve *2* as compared to curve *1*. The different behaviours of curves *1* and *2* in Fig. 2 points out to the presence of a noticeable space charge in the drift space even after switching-off the beam injection pulse. Indeed, only the presence of trapped electrons, which drift for a comparatively long time in the magnetic field and whose effect is essential in 400 ms after the injection pulse end, may explain the reverse hysteresis on the I_{ex} versus I_{in} dependence, curve *1* in Fig. 2. When the beam of 400 μs in duration with the 400-μs pause between pulses is injected, the drift space cannot be freed, due to inertia, from the space charge accumulated during the previous current pulse. The time-averaged distribution functions of the incident, passing, and reflected beams, which were measured under these conditions, have a spread over

553
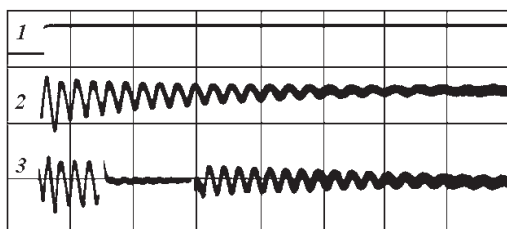
Fig. 3. Oscillograms: *1* — a negative voltage pulse at the electron gun cathode; *2* — current on one of the π-electrodes; *3* — the same as in *2*, but with the 0.3-ms positive pulse of the 1-V amplitude on the second π-electrode (2 ms sweeps)

Fig. 4. Spatial distribution of the potential in longitudinal direction, the beam current being equal to 10 mA (*1*), 17 mA (*2*), and the amplitude of diocotron oscillations (*3*), B=1000 Oe, U_B=30 V, τ=1 ms

longitudinal velocities $\frac{\Delta v}{v_{dr}} \approx 0.7 \div 0.8$. Figure 3 shows the oscillograms of the negative voltage on the electron gun cathode (curve *1*); the current on the π-electrodes (curve *2*); and the current on the same π-electrode when a positive pulse of 0.3 msec in duration and of the 1-V amplitude is applied to the other electrode (curve *3*). The oscillations registered with the π-electrode correspond to the diocotron branch of charged plasma oscillations with the azimuthal wave number l=1. It is easily seen from Fig. 3 that the noticeable "tail" of oscillations exists during more than 1 ms after the end of the beam injection pulse. It is also seen that the oscillation period increases with time, and the times of growth and disruption of oscillations do not exceed their period, as it follows from oscillogram *3* in Fig. 3 where the positive pulse is applied to one of the π-electrodes for the demonstration of this fact. The pulse with the 1-V amplitude totally damps the "tail" oscillations during its period of 0.3 ms. Our experiments show that the diocotron mode of oscillations with l=1 is excited, as a rule, also during the beam injection, the frequency of these oscillations being always higher than the frequency of "tail" oscillations. The presence of diocotron oscillations points out that, in the drift space apart from the beam electrons passing through it, the electrons are present with the lifetime not less than the diocotron oscillation period to excite these oscillations at all.

The presence of these "tails" on oscillograms in Fig. 3 confirms that the lifetime of the part of electrons is considerably larger than the period of the l=1 diocotron mode. Using the relation for the drift frequency of a rotating hollow beam in the crossed own electrical and longitudinal magnetic fields $\omega = \frac{b}{2}\left(\omega_{pe}^2/(2\omega_{He})\right)$ $b \approx 0.5$, $H = 1$ kOe under our experimental conditions), one can estimate the electron density n_e with the help of oscillograms of Fig. 3 as follows: $n_e \approx 4 \times 10^6$ cm^{-3}. The particle density of the injected beam is $n_b \approx 2 \times 0^7$ cm^{-3}.
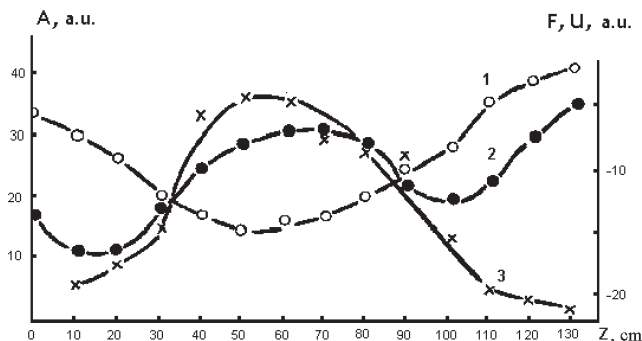
This estimate shows that a fraction of electrons drifting for a long time $\tau \sim 1$ ms in the magnetic field is noticeable and amounts to $n_e/n_b \approx 0.2$.

The spatial distributions of potential in the direction of movement of particles along the magnetic field are presented in Fig. 4. The distributions were taken with the HF probe, the probe at a floating potential.

For the beam current $I_B \leq I_{Cr} \approx 15$ mA, the potential distribution in the longitudinal direction has a typical form for velocity-spread electron beams, i.e. the distribution of the "bell" type (curve *1*). Such potential distribution leads to the accelerated loss of electrons from the drive space caused by the electric fields of the space charge of the beam. The radial localizations of the direct and reverse flows of electrons in the drive space coincide. The beam current being increased, $I_B \geq I_{Cr}$, the potential form in the drive space essentially changes with the formation of a potential pit for electrons at the drive space center (curve *2*).

A transformation of the potential distribution in the longitudinal direction is accompanied by the excitation of oscillations of the beam density which have been identified in [9] as the diocotron oscillations with the l=1 mode. In Fig. 4, the distributions of diocotron oscillations in the drive space are seen to correlate with the spatial localization of the potential pit (curve *3*).

3. Theoretical Model

The theoretical description of the phenomena denoted in Section 2 may be made within the framework of the following model. We consider the hollow electron beam which is contained in a cylindrical waveguide with
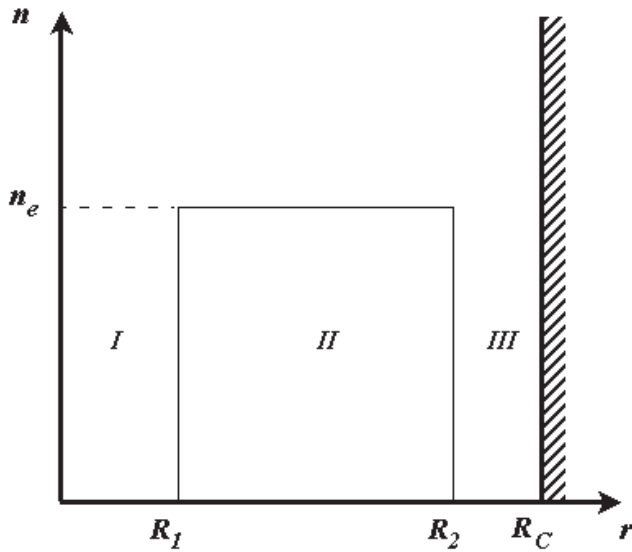
Fig. 5. Profile of the electron beam density. R_1 and R_2 — inner and external electron beam's radii, R_c — waveguide wall, and n_e — unperturbed electron density

Fig. 6. Experimental (*1*, *2*) and qualitative theoretical dependences (*3*) of a voltage drop on the radius. Beam current 10 mA (*1*) and 17 mA (*2*)

superconductive walls in an external constant magnetic field $\vec{H}_0 \uparrow\uparrow \vec{e}_z$. The profile of the electron beam density distribution function is shown in Fig. 5. The unperturbed beam velocity is constant and equals v_{z0} in the axial direction.

It is obvious that such a beam will be subjected to the diocotron instability because of a shear of the medial angular velocity which exists in the system [5]. However, it is possible to select such a profile of the electric field, at which the beam will make motion with a constant value of the angular velocity $\Omega = $ const. For this purpose, it is necessary that the electric field intensity E linearly depend on the radius r in the field of II. Such a dependence corresponds to the system including two surface charges of opposite signs (the first charge, $\sigma_1 = -(en_e R_1)/2$, is located on the interior border of a beam $r = R_1$, the second one, $\sigma_2 = (en_e R_2^2)/(2R_c)$, is located on the wave guide wall $r = R_c$). Thus, in the system consisting of a hollow beam and two surface charges σ_1 and σ_2, the medial angular velocity is constant $\Omega = \frac{\omega_e}{2}\left[1 \pm \sqrt{1 - (2\Omega_e^2)/\omega_e^2}\right]$ ($\omega_e = (eH)/(m_e c)$ is the Larmor frequency, and $\Omega_e^2 = (4\pi e^2 n_e)/m_e$ is the electron plasma frequency), and the diocotron instability will not develop.

One can see that, at such allocation of charges, the potential in the region 1 should be constant. Therefore, without any loss of generality, the field 1 can be counted both as a vacuum and as a metal as well. The

last statement corresponds to the general expedients of producing of hollow beams.

In Fig. 6, the experimental dependences of a voltage drop on the radius are given (curves *1* and *2*) relatively to the above-stated theoretical assumptions (curve *3*) concerning surface charges.

The dispersion equation featuring the propagation of electrostatic waves in a cold electron hollow beam is possible to obtain from the equations of magnetohydrodynamics using the approach enunciated in [5]. Considering small harmonic additives to the velocity $\vec{v}$, potential φ, and density n_e, it is possible to easily obtain the equation

$$\left\{\left[\varepsilon_1 \kappa_2 R_1 \frac{J_l'(\kappa_2 R_1)}{J_l(\kappa_2 R_1)} - \kappa_2 R_1 \frac{I_l'(\kappa_2 R_1)}{I_l(\kappa_2 R_1)} - l\varepsilon_2\right] \times \right.$$

$$\times [J_l(\kappa_2 R_1) N_l'(\kappa_2 R_2) - J_l'(\kappa_2 R_2) N_l(\kappa_2 R_1)]\kappa_2 R_2 \Bigg\} \Bigg/$$

$$\Bigg/ \left\{ \frac{J_l(\kappa_2 R_2)}{J_l(\kappa_2 R_1)} \frac{\kappa_1 R_2}{G(R_2, R_c)} \left[K_l(\kappa_1 R_c) I_l'(\kappa_1 R_2) - \right.\right.$$

$$- K_l'(\kappa_1 R_2) I_l(\kappa_1 R_c)\Big] +$$

$$+ \left[l\varepsilon_2 \frac{J_l(\kappa_2 R_2)}{J_l(\kappa_2 R_1)} - \varepsilon_1 \kappa_2 R_2 \cdot \frac{J_l'(\kappa_2 R_1)}{J_l(\kappa_2 R_1)}\right]\Bigg\} =$$
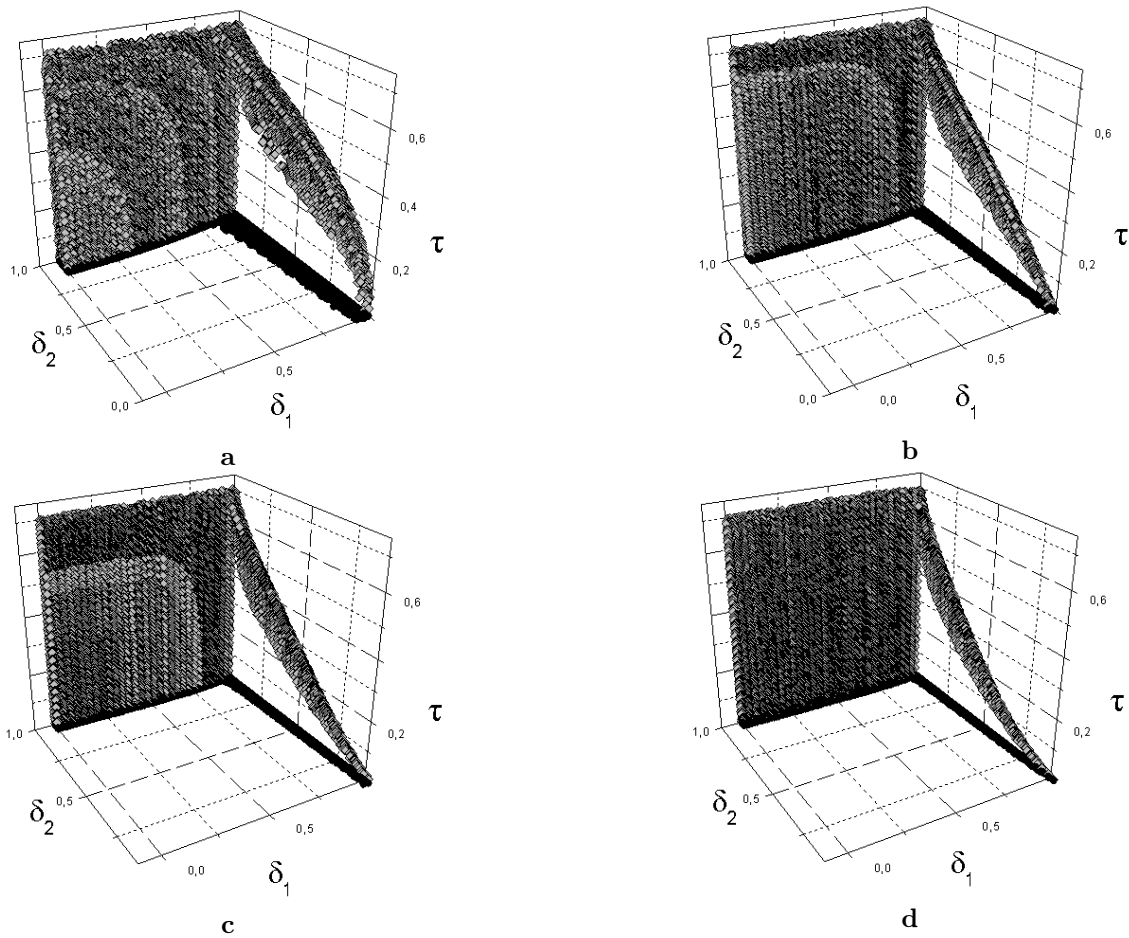
Fig. 7. Areas of stable oscillations in the space of parameters $\delta_1 = \frac{R_1}{R_2}$, $\delta_2 = \frac{R_2}{R_c}$ and $\tau = \frac{\Omega_e}{\omega_e}$ for different values of the azimuthal wave number l. a, b, c, d correspond to $l = 1,\ 2,\ 3,\ 4$, respectively

$$= \varepsilon_1 \kappa_2 R_1 [J_l (\kappa_2 R_2) N_l' (\kappa_2 R_1) - J_l' (\kappa_2 R_1) N_l (\kappa_2 R_2)]+$$

$$+ \kappa_1 R_1 [J_l (\kappa_2 R_1) N_l (\kappa_2 R_2) - J_l (\kappa_2 R_2) N_l (\kappa_2 R_1)] \times$$

$$\times \frac{I_l' (\kappa_1 R_1)}{I_l (\kappa_1 R_1)} + l \varepsilon_2 \big[J_l (\kappa_2 R_1) N_l (\kappa_2 R_2) -$$

$$- J_l (\kappa_2 R_2) N_l (\kappa_2 R_1) \big], \tag{1}$$

where $G(R_2, R_c) = K_l (\kappa_1 R_c) I_l (\kappa_1 R_2) - K_l (\kappa_1 R_2) \times$ $\times I_l (\kappa_1 R_c)$, $J_l(x)$, $N_l(x)$, $I_l(x)$, and $K_l(x)$ are the Bessel functions, Neumann functions, modified Bessel functions, and Macdonald functions, respectively, and l is the order of a relevant special function. The following notations are also introduced:

$$\varepsilon_1 = 1 - \frac{\Omega_e^2}{(\omega - l\Omega - k_z v_{z0})^2 - (\omega_e - 2\Omega)^2},$$

$$\varepsilon_2 = \frac{\Omega_e^2 (\omega_e - 2\Omega)}{(\omega - l\Omega - k_z v_{z0}) \left[(\omega - l\Omega - k_z v_{z0})^2 - (\omega_e - 2\Omega)^2 \right]},$$

$$\varepsilon_3 = 1 - \frac{\Omega_e^2}{(\omega - l\Omega - k_z v_{z0})^2},$$

$\kappa_1 = \kappa_3 = k_z$, $\kappa_2^2 = k_z^2 \frac{\varepsilon_3}{\varepsilon_1}$, where k_z is the longitudinal wave number, l is the azimuthal wave number. Hatches in Eq. (1) mean the derivatives with respect to the argument of the appropriate higher transcendental function, for example, $\frac{dJ_l(\kappa_i r)}{d\kappa_i r}\Big|_{r=R_i} = J_l' (\kappa_i R_i)$. Equation (1) relates the oscillation frequency ω to the azimuthal wave number k_z, longitudinal wave number l, and the parameters R_1, R_2, R_c, ω_e of the equilibrium state.

In the case of long-wave oscillations ($k_z = 0$) considered in experiments, Eq. (1) takes the form

$$\frac{2\left(1 + \varepsilon_2 - \varepsilon_1\right)}{\left[\frac{(R_2/R_c)^{2l}+1}{(R_2/R_c)^{2l}-1} - (\varepsilon_2 - \varepsilon_1)\right]} = (R_2/R_1)^{2l}\left((R_1/R_2)^{2l} - 1\right) \times$$

$$\times \left(\varepsilon_1 \frac{(R_1/R_2)^{2l}+1}{(R_1/R_2)^{2l}-1} - 1 - \varepsilon_2\right). \qquad (2)$$

Let's note that Eq. (2) in extreme cases, i.e. in the limit $R_1 \to 0$ or $R_2 \to R_c$, describes the dispersion properties of a plasma cylinder or a plasma pipe, respectively [5].

Equation (2) is the sixth-order equation for the frequency ω. Therefore, its analytical solution is not obviously available. However, it is possible to numerically determined values of such parameters as R_1/R_2, R_2/R_c, Ω_e/ω_e, at which the development of an instability is possible.

In Fig. 7, the areas of stability in the space of the parameters R_1/R_2, R_2/R_c, Ω_e/ω_e are given for various values of the azimuthal wave number l. The algorithm of areas of stability is as follows: at the fixed values R_1/R_2, R_2/R_c, Ω_e/ω_e, the relevant frequencies were determined. In the case when all the solutions were real ($\mathrm{Im}\,\omega = 0$), the relevant point was mapped in the space (for presentation, black colour in Fig. 7 shows the stability area projections onto the $\delta_1\delta_2$-plane). It is apparent from Fig. 7 that stable oscillations occur in an electron plasma hollow beam in those areas, where the Larmor frequency ω_e is much higher than the plasma frequency Ω_e, and the beam external radius differs slightly from the radius of the wave guide. In addition, the relative share of stable oscillations (the ratio of the volume of areas where the stable solutions exist to the volume of space $\delta_1\delta_2\tau$) decreases with increase in l. It is also possible to plot the area of existence of quasi-stable ($\mathrm{Im}(\omega)/\mathrm{Re}(\omega) << 1$) oscillations. In Fig. 8, the area of solutions with $\mathrm{Im}(\omega)/\mathrm{Re}(\omega) \approx 10^{-3}$ is given. Though, such oscillations are unstable; however, their increment is much less than the oscillation frequency.

The existence of quasi-stable oscillations may explain, in our opinion, a series of experiments [3, 9, 11] stated in Section 2, in which the electron beam (with $\delta_1, \delta_2 \sim 1$ and $\tau << 1$) exists the enough long time ($\tau \sim 10^{-3}$ s) much exceeding that required for the diocotron instability development, $\tau_D \sim 10^{-5}$ s.
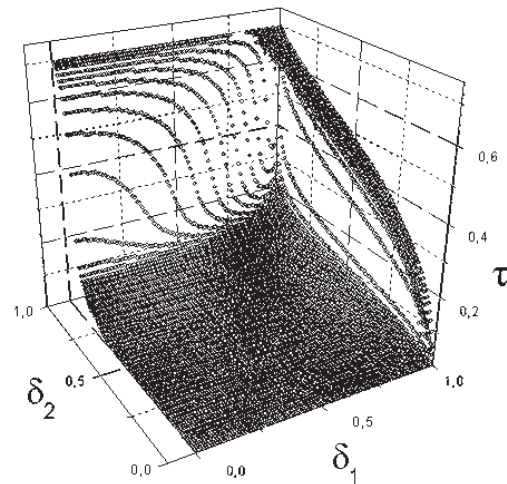
Fig. 8. Area of quasi-stable ($\mathrm{Im}(\omega)/\mathrm{Re}(\omega) << 1$) solutions for the $l=1$ mode (quasi-stable oscillations take place in the area below the surface)

4. Conclusions

Thus, we come to the conclusion that, when electron beam with a large velocity spread is injected, the long-lifetime electrons are accumulated in the drift space located in the magnetic field, the accumulated density of particles being a noticeable fraction of the injected electron beam density.

It is experimentally proved that:

a) oscillations of non-neutral particles in the drive space have diocotron nature.

b) oscillations are localized in the drive space along the axial direction.

c) oscillations exist for aa rather long time, 10 msec, after the impulse termination. That may be caused by the capture of slow particles during the injection.

The theoretical explanation of the experimental results mentioned above can be given within the framework of the model considering a tubular electron beam with constant density profile. The dispersion equation obtained under the assumption of the shearless rotation of a tubular beam predicts the existence of stable oscillations in cases where the external beam boundary is close to a wave guide wall. It is shown that, with increase in the azimuthal wave number l, the relative share of stable oscillations of an electron plasma tubular beam decreases. It is shown that, at small densities of electrons, the existence of quasi-stable oscillations is possible. The theoretical estimation of the lifetime of entrapped particles in the case of quasi-stable

oscillations $\mathrm{Im}(\omega)/\mathrm{Re}(\omega) \approx 10^{-3}$ demonstrates a good agreement with the experimental results.

1. *Malmberg J.H., O'Neil T.M., Hyatt A.W., Driscoll C.F.*//Proc. 1984 Sendai Sumposium of Plasma Nonlinear Phenom., 1984. — P.31.

2. *Bollinger J.J., Wineland D.J.* // Phys. Rev. Lett. 1984. **53**. P.348.

3. *Bizyukov A., Volkov E.D., Tarasov I.K.*// Problems of Atomic Science and Technology, 2002, N 4, series Plasma Physics (7). — P.146—148.

4. *Malmberg J.H., Driscoll C.F.* // Phys. Rev. Lett. 1980. **44**. P.654.

5. *Davidson R.C.* Theory of Nonneutral Plasmas. Reading. — MA: Benjamin, 1974.

6. *Finn J.M. et al.* // Non-neutral plasma physics III, AIP Conference Proceedings, Princeton, New Jersey, August 1999. — P.198—207.

7. *Kabantsev A.A., Driscoll C.F.* // Non-neutral Plasma Physics III, AIP: Conf. Proc., Princeton, New Jersey, August 1999. — P.208—213.

8. *Gianni G.M. et al.* // Ibid. — P.129—134.

9. *Krivoruchko S.M., Tarasov I.K.* // Plasma Phys. Repts. **19 (11)**, Nov. 1993.

10. *Atkinson H.H.* //1962a, Proc. 4th Intern. Congress on Microwave Tubes, September, 1962 Eindhaven: Centrex, 1963. — P.559.

11. *Bizyukov A.A., Volkov E.D., Tarasov I.K.* // Problems of Atomic Science and Technology, 2002, N 4, series Plasma Physics (7). — P.144—145.

СТІЙКІСТЬ ЕЛЕКТРОННОГО ПУЧКА ІЗ СИЛЬНИМ РОЗКИДОМ ЗА ШВИДКОСТЯМИ У САМОУЗГОДЖЕНІЙ ПАСТЦІ ПЕННІНГА—МАЛМБЕРГА

В.І. Лапшин, І.К. Тарасов, І.В. Ткаченко, В.І. Ткаченко

Р е з ю м е

Експериментально і теоретично досліджено процес накопичення та утримання заряджених частинок під час інжекції трубчастого електронного пучка, що є розмитим за швидкостями. Пучок було інжектовано у камеру дрейфу, що перебувала у сильному зовнішньому поздовжньому магнітному полі. Експериментально доведено, що під час інжекції формується колективна самоузгоджена електронна пастка. Під час формування вона захоплює електрони пучка і утримує їх у просторі камери дрейфу. Існування колективної самоузгодженої пастки (останню стадію експерименту) теоретично можна пояснити за допомогою моделі, що розглядає еволюцію безширової ротації трубчастого електронного пучка. Аналітично отримано дисперсійне рівняння для такого пучка та проведено оцінку утримання заряджених частинок у пастці. Для цього у просторі параметрів експерименту було побудовано поверхні, що відокремлюють нестійкі коливання від стійких. Результати теоретичних досліджень добре узгоджуються із експериментом.